

Manuscript details

Manuscript number

HE_2016_1172

Title

GELATIN AS A PROMISING PRINTABLE
NUTRIENT FEEDSTOCK FOR MICROBIAL
FUEL CELLS (MFC)

Article type

Full length article

Abstract

The Microbial Fuel Cell (MFC) is an energy transducer technology that can directly produce electricity from bacterial oxidation of organic matter. MFCs consist of two reaction chambers (anode and cathode) separated by a semipermeable membrane. This study describes the work carried out towards the optimization of critical MFC components, with potential 3D fabricated materials. The response of the optimized fuel cells, which were fed with soft materials such as gelatin, alginate and Nafion is also reported. The optimized components were the membrane and the cathode electrode. A traditional Nafion membrane was substituted with a custom made terracotta sheet and the electrode used was a single sheet of carbon veil coated with an activated carbon paste. The results showed that among the soft materials tested within the anodic chamber, gelatin performed the best; it also revealed that even after a 10-day starvation period gelatin demonstrated better longevity. These results show that MFCs have the potential to be 3D-printed monolithically using the EVOBOT platform.

Highlights

- Soft materials tested for the first time as feedstock in MFCs
- Higher output from gelatin fed MFCs after constant feeding stopped
- Detrimental effect of liquid Nafion to the microbial community
- Potential implementation of the proof of concept to EVOBOT platform for 3D printed MFCs

GELATIN AS A PROMISING PRINTABLE NUTRIENT FEEDSTOCK FOR MICROBIAL FUEL CELLS (MFC)

Ioannis Ieropoulos^{a,b,*}, Pavlina Theodosiou^a, Benjamin Taylor^a, John Greenman^b and Chris Melhuish^a

^a Bristol BioEnergy Centre, Bristol Robotics Laboratory, University of the West of England, Bristol BS16 1QY, UK

^b Biological, Biomedical and Analytical Sciences, University of the West of England, BS16 1QY (UK)

* Corresponding Author: email: ioannis.ieropoulos@brl.ac.uk

Bristol BioEnergy Centre, Bristol Robotics Laboratory, University of the West of England, Bristol BS16 1QY, UK

Abstract

The Microbial Fuel Cell (MFC) is an energy transducer technology that can directly produce electricity from bacterial oxidation of organic matter. MFCs consist of two reaction chambers (anode and cathode) separated by a semipermeable membrane. This study describes the work carried out towards the optimization of critical MFC components, with potential 3D fabricated materials. The response of the optimized fuel cells, which were fed with soft materials such as gelatin, alginate and Nafion™, is also reported. The optimized components were the membrane and the cathode electrode. A traditional Nafion membrane was substituted with a custom made terracotta sheet and the electrode used was a single sheet of carbon veil coated with an activated carbon paste. The results showed that among the soft materials tested within the anodic chamber, gelatin performed the best; it also revealed that even after a 10-day starvation period gelatin demonstrated better longevity. These results show that MFCs have the potential to be 3D-printed monolithically using the EVOBOT platform.

Keywords MFC, EVOBOT, Gelatin, 3D-printing, Nutrient feedstock

1. Introduction

The microbial ability to decompose organic matter and liberate electrons as part of their metabolic pathways has been proven beneficial for the development of microbial fuel cells (MFCs), which emerged more than 100 years ago [1]. Microbial fuel cells (MFCs) can be defined as energy transducers, which convert chemical energy stored in organic matter into electricity through bacterial utilisation [2]. The electrical output from MFCs is due to the bacterial catalytic conversion, which occurs in the anode. MFCs consist of two compartments, the positive cathode and the negative anode; each compartment has its own electrode which acts as the electron sink (anode) and electron acceptor (cathode) of the cell [3]. The two parts are separated by a semi-permeable membrane allowing the protons generated in the anode, from the bacterial oxidation of the organic molecules, to flow through to the cathode. Electrons flow through an external connecting wire or circuit, which facilitates current flow. Both electrons and protons are re-combined at the cathode side with dissolved oxygen to form H₂O as the by-product [4]. Due to these distinct characteristics MFCs are often described in the literature as biological batteries or bio-batteries [5]. MFCs

42 have a great potential as a new green source of energy, since many types of organic
43 substrates can be utilised; use of MFCs in wastewater treatment processes can potentially
44 reduce treatment costs and pollution, as well as generate on site electricity.

45 The 3D printing technology was first proposed in the 1980s [6] and since then it is driving
46 major innovations in many sectors including food industry [7], cell biology [8] and
47 pharmaceuticals [9]. MFC technology and 3D printing (rapid fabrication) were interlinked in
48 2010 where compartments of MFCs were fabricated and tested over Perspex material
49 showing the advantages of 3D printed compartments, not only in accelerating the assembly
50 process but also reducing the internal resistance of MFCs [10]. Many improvements have
51 been achieved in the field of MFCs due to 3D printing including the fabrication of Nanocure®
52 MFCs and their implementation on autonomous robots [11] as well as the emergence of new
53 designs for easy assembly, such as twist n' play MFCs [12]. The era of 3D printing opened
54 new roads for the improvement of MFCs' core materials such as 3D printed, ion exchange
55 membranes [13] and electrodes [14].

56 It is aimed to develop monolithically 3D fabricated MFCs through the EVOBOT platform [15].
57 To facilitate the monolithic 3D fabrication process of the MFC, essential MFC components
58 such as membrane, electrodes and even feedstock need to be optimised. The cells
59 employed in this study had open-to-air cathodes with micro porous layer (MPL) and coated
60 carbon veil as the cathode electrode. MPL is an activated carbon paste which is able to be
61 extruded from the platform. A custom made, potentially extrude-able, single layer of
62 terracotta clay was used as a semi-permeable membrane.

63
64 The materials tested were selected based on their properties, as these are critical at
65 ensuring that maximum growth conditions are maintained within the MFCs, which will result
66 in maximum power output performance levels. The ideal substratum has to have (a) the
67 appropriate porosity, which will facilitate both access to the electrode surface for the
68 microbes and free percolation of the liquid medium to reach all the colonized parts and (b)
69 the appropriate conductivity, in order to encourage optimum surface reactions, between the
70 microbial cells and the electrode surface. This is the key mechanism that maintains a fixed
71 thickness biofilm on a given surface area of electrode material, since this direct conductance
72 of electrons (charge transfer) is the primary mechanism of bacterial survival, under
73 anaerobic conditions. The electrode surface acts as the end-terminal electron acceptor,
74 which the microbes need (instead of e.g. oxygen) to anaerobically respire. The material must
75 also be biocompatible, chemically inert, long-life and with a good structural integrity.

76
77 This study presents the results from MFCs' fed for the first time with soft materials (gelatin,
78 alginate as a nutrient feedstock) and Nafion® as a negative control. The aim of the study
79 was to test the power output response and the behaviour of the MFCs by feeding them with
80 these different soft materials, which can all be potentially extruded from the EVOBOT
81 platform.

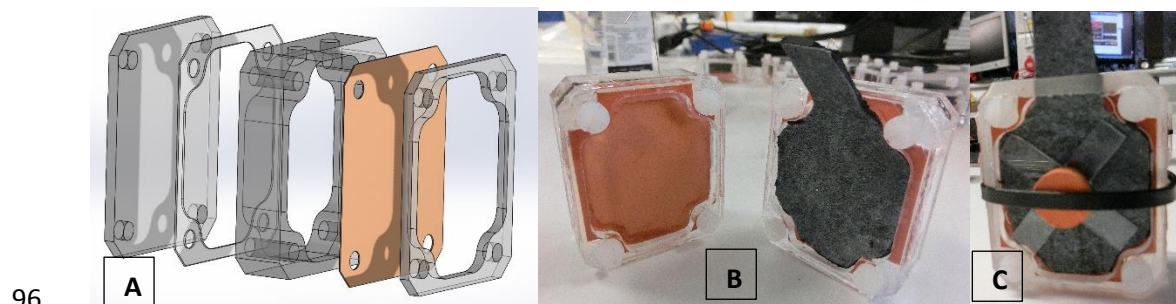
82

83 **2. Materials and Methods**

84

85 **2.1 MFC design**

86 Twelve analytical size, cubic MFCs were employed for this experiment. The MFC chambers
87 were laser cut from Polymethyl methacrylate (Perspex) sheets (**Fig. 1A**). The cathode
88 chamber was removed completely, in order to form an oxygen cathode MFC, and replaced
89 with a Perspex framework, which sandwiched the 6 x 5 cm terracotta membrane (2mm
90 thickness) with the 25 mL anode chamber (**Fig. 1B**). A thick layer of silicone was deposited
91 between the anode chamber and the cathode framework, which acted as a 'cushion' for the
92 ceramic membrane, when bolted together. The screws used for the assembly were 5 mm
93 nylon studding and nuts. The whole cells were then partially wrapped with Parafilm® M
94 Sealing Film to ensure that the moisture was retained in the open-to-air cathode side (not
95 shown in the figure).



96 **A** **B** **C**
97 **Fig. 1 – A. Computer aided design (CAD) of the optimised MFCs. B. Clay membrane**
98 **and the attached MPL electrode. C. Open to the air cathode construction**

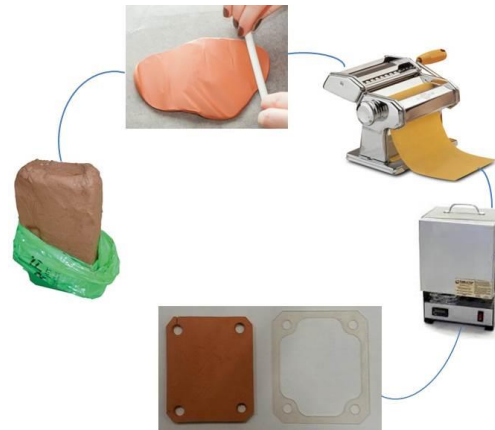
99 2.2 Electrode Materials

100 Anode electrodes were constructed from untreated (catalyst free) carbon veil fibre, with
101 30g/m^2 carbon loading (PMF Composites, Dorset, UK) and a total surface area of 270 cm^2 .
102 The anode electrode was folded down five times, until the projected surface area was 8.45
103 cm^2 and was able to fit into the anodic half-cell (30 cm^2). A piece of nickel wire,
104 approximately 10 cm in length, was pierced through the electrode to provide the connection
105 point with the data logger and external load crocodile clip. The cathode electrode was made
106 of two layers; a gas diffusion layer (GDL) and a microporous layer (MPL). The GDL was a
107 single sheet of the same carbon veil material used for the anode electrode but coated with
108 30% polytetrafluoroethylene (PTFE) (Sigma Aldrich, UK). The sheet was left to dry for 24
109 hours in room temperature, and once the GDL dried the activated carbon paste was applied
110 on top to form a thick layer of MPL (2 mm). The MPL was a mixture of activated carbon
111 powder (G.Baldwin & Co., London, U.K.) blended with PTFE in a 4:1 ratio and deionised
112 water (120 mL). The activated carbon paste was then hot pressed, using a household iron
113 [16], and subsequently heated for 15 minutes to $200\text{ }^\circ\text{C}$ to allow MPL liquefaction. The
114 cathode electrode sheet was directly attached onto the exposed membrane but in order to
115 ensure the electrode-membrane contact, a thin (0.5 mm) Perspex cross was pressed against
116 the electrode using a cut-to-shape cork (**Fig. 1C**) that was tightened with a cable tie.

117 2.3 Membrane preparation

118 Red terracotta earthenware clay was used for the membrane fabrication. The terracotta was
119 worked with a pastry roller in order to remove air bubbles and until it reached 5 mm of
120 thickness (**Fig.2**). Then, it was processed using a pasta making machine until it reached 2.5
121 mm thickness. The flat sheet was then cut to size (6 x 5 cm) and placed between two sheets

122 of wood to absorb the moisture and dried for 12 hours. The membranes were then kilned at
123 a temperature of 1070 °C, which cured the materials through structural bonding of the clay.



124

125 **Fig. 2 – In-house preparation technique for custom made clay membrane**

126

127 **2.4 Inoculation process and load condition**

128 Activated sludge, which was supplied by the Wessex Water Scientific Laboratory (Saltford,
129 UK) was used as the initial inoculum. The sludge (25 mL) was injected manually into the
130 sterile chamber and the experiment initially started in batch mode, but then turned into
131 continuous flow. Three sludge exchanges occurred in the first three days of the experiment
132 by emptying the chamber and re-filling it with fresh inoculum. For the next three batch mode
133 feedings the inoculum used was sludge with tryptone (1%) and yeast extract (0.5%) (TYE)
134 as a background nutrient solution, fed at a final concentration of 1:10. Due to inherent
135 absorption/evaporation processes, the experiments turned into continuous flow on the 18th
136 day of the experiment. The flow rate of the constant pumping was 0.5 rpm (4.2 mL.h⁻¹) and
137 the hydraulic retention time (HRT) was 7.77 h. The feeding regime was full strength (1.5%)
138 TYE.

139 One hour after the first inoculation, once the open circuit cells performance reached a
140 plateau, an external load of 2.7 kΩ was connected and this remained unchanged until the
141 end of the experiment.

142 **2.5 Feeding regime and process**

143 After 18 days of sole 1.5% TYE feeding the triplicates of MFCs were fed with water-soluble
144 pork-derived gelatine powder (240 Bloom Type A, MM ingredients, UK) , sodium alginate
145 (pure powder, Minerals Water, UK) and as a negative control, liquid Nafion® perfluorinated
146 resin solution (Sigma Aldrich, UK). TYE (1:10) was also used as a background solution in all
147 experiments. To ensure that the same weight of nutrients was added, the final concentration
148 of the target material into the solution was 2%. This concentration was selected after testing
149 different ratios in order to obtain a liquid state with sufficient low viscosity that will enable it to
150 be pumped through the tubes without causing blockage. The control triplicate was fed with
151 neat human urine and 1:10 TYE background solution, where pooled urine was obtained from
152 anonymous healthy individuals. The cells were fed in continuous flow and this was
153 maintained using a 16-channel peristaltic pump (205U, Watson Marlow, Falmouth, UK) with
154 a flow rate of 0.5 rpm (4.2 mL.h⁻¹).

155 2.6 Data recording and analysis

156 For the data collection, MFC output was recorded in millivolts (mV) against time using
157 Agilent Keysight 34970A Data Acquisition / Data Logger Switch Unit (Keysight Technologies,
158 UK) with a 3 min sample rate. Data were processed and analysed using MS Office Excel
159 and GraphPad Prism® version 5.01 software package (GraphPad, San Diego, California,
160 U.S.A).

161 Current (I) in amperes (A) was calculated using Ohm's law, $I = V/R$, where V is the
162 measured voltage and R is the known value of the external resistive load in ohms (Ω). Power
163 (P) in watts (W) was calculated by multiplying voltage with current: $P = I \times V$ [17].

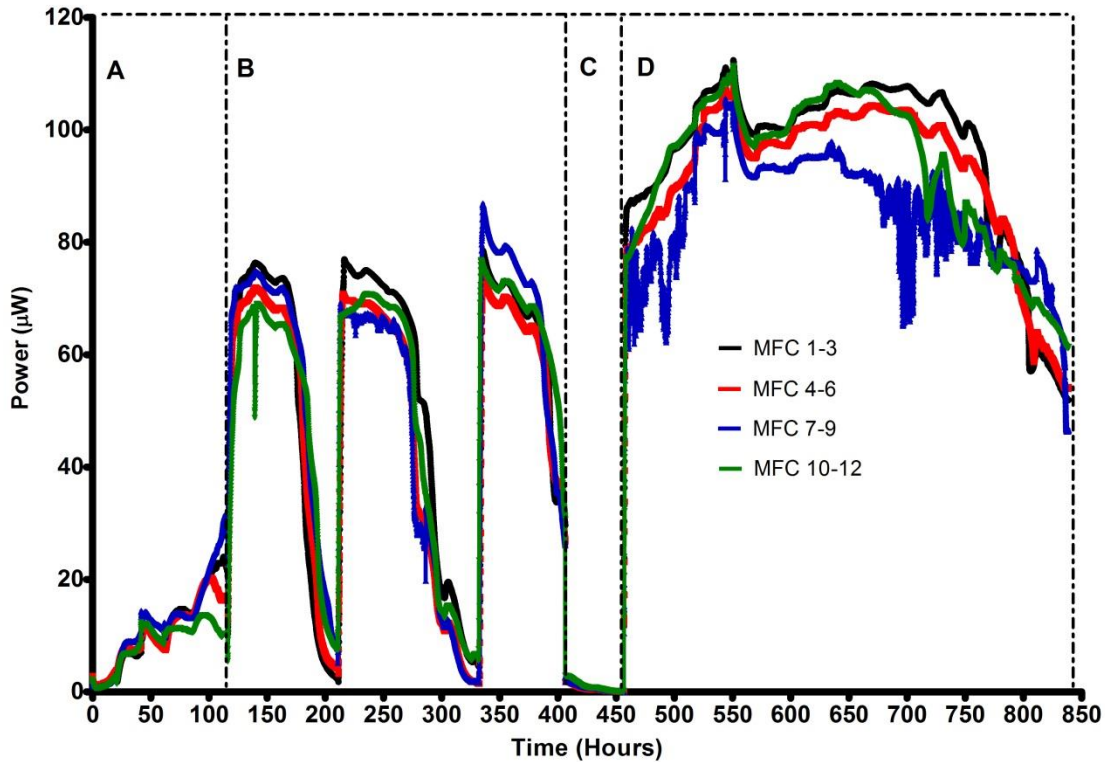
164 2.7 Polarization Experiment

165 Polarization experiment was performed using a resistorstat device, by sweeping 37 resistor
166 values covering the range of 3.74 Ω - 30 k Ω [18]. The resistance load was changed every 3
167 minutes; however data recording occurred every 30 seconds (6 readings per load value).
168 Polarization curves were generated from the collected data.

169 3. Results

170 3.1 Batch mode inoculation period and continuous flow operation

171 The power output obtained from the microorganisms' inoculation procedure with neat sludge,
172 is highlighted in **Fig. 3A**. The loaded cells were able to develop a visibly dense biofilm over
173 the electrode, which gave approximately 20 μ W of power output. After the inoculation and
174 colonisation phase, once the electrode biofilm was exposed to sludge in 1.5% TYE (1:10),
175 the power output was increased by three-fold (**Fig.3B**). Although the performance of the
176 cells was consistent and repeatable, a high evaporation loss caused the anode chamber to
177 dry within 96 hours, leaving behind semi solid sediment at the bottom of the chamber, and
178 having a deteriorating effect on the performance of the cells. An almost zero power
179 performance was recorded after the anode chamber was left to dry out completely (**Fig. 3C**).
180 As can be seen from **Fig. 3D**, once the cells turned to continuous flow operation, the power
181 output increased by 0.4-fold. **Fig. 3** shows the consistency of the twelve cells' behaviour
182 when all of them were fed with the same feedstock at the same flow rate.



183

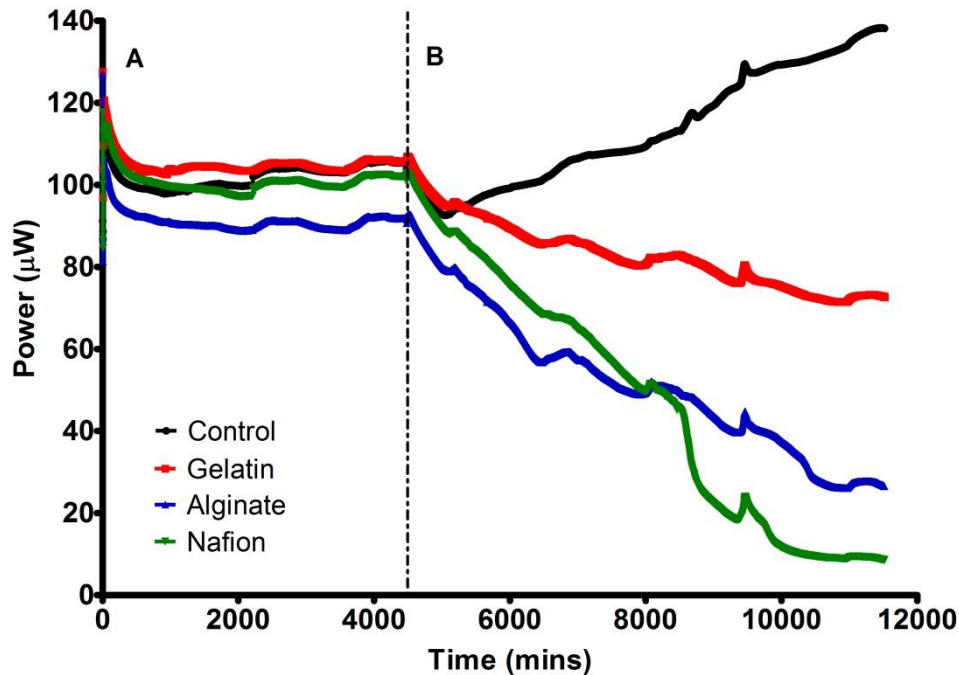
184 **Fig.3 - Power profile of the inoculation process and initial feeding of the twelve MFCs**

185 Area A represents the batch mode inoculation period of the fuel cells with neat sludge. In
 186 area B the cells were fed with TYE and sludge (1:10). The power decrease was related with
 187 the absorption loss of anolyte liquid, due to the clay membrane. Area C highlights the total
 188 dry period of the cells while area D shows the behavior of the cells after turned into
 189 continuous flow.

190 **3.2 Initial Response of cells fed with soft materials**

191 After feeding the 12 MFCs with TYE for 18 days, the two triplicate groups, namely MFCs 4-6,
 192 and MFCs 7-9, were fed with the target polymeric feedstock substrates gelatin and alginate,
 193 respectively, whereas and MFCs 10-12 were fed with the negative control, Nafion. MFCs 1-3
 194 were fed with the positive control urine medium. Even though the feedstock switching had a
 195 slight decreasing effect on the MFC power output for the first 10 hours, after this period the
 196 performance levels began to diverge (**Fig. 4B**). The profile of the first 5 days showed that the
 197 urine fed MFCs' performance improved, compared with the soft material fed MFCs whose
 198 performance decreased. Similar decreasing profiles were identified from alginate and
 199 gelatin, with the only difference being that gelatin was more than two-fold higher in power
 200 performance than alginate. A possible explanation for the superiority of gelatin over alginate
 201 is the difference in the calorific value of the two substances (gelatin: 329 kCal/100g –
 202 alginate: 248 kCal/100g). As stated in section 2.5 the dilution of the compounds was
 203 standardised based on their viscosity and not their calorific value. As shown in **Fig.4**, the
 204 performance from the Nafion fed MFCs deteriorated rapidly over time.

205



206

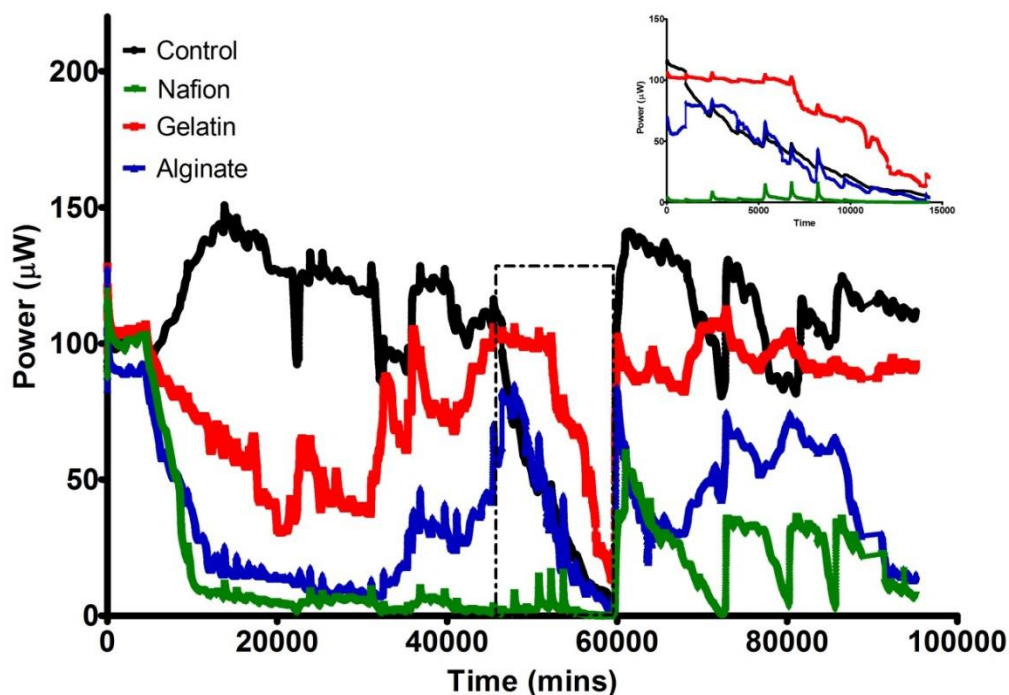
207 **Fig. 4 - Time profile of MFC's response after feeding with soft materials for the first**
 208 **time.**

209 The last three days of the 18-day period is presented in the graph (area A) followed by the
 210 response once the feedstock changed (area B). The fuel cells were fed with 1.5% TYE for
 211 the first 18 days, and then target soft materials added. Gelatin outperformed the other soft
 212 materials ($p < 0.0001$).

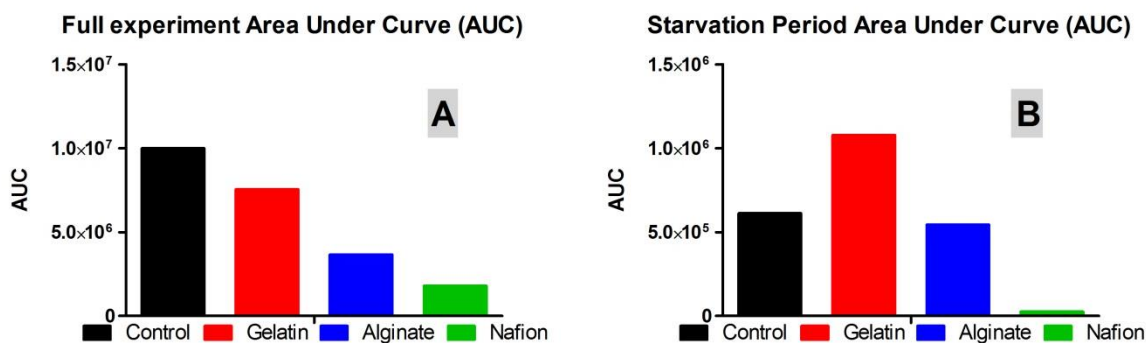
213 3.3 Overall performance and starvation period of the cells

214 The average power production of the MFCs fed with different soft materials is shown below
 215 (**Fig. 5**). The data were consistent with the initial response to the change of feedstock. The
 216 urine fed control MFCs remained the highest in power output with the maximum being
 217 149.23 μW ; gelatin followed as the second best with a maximum power at 111.26 μW . The
 218 performance is represented also as area under curve shown in the graph of **Fig. 6A**.

219 While constant pumping was supplied to the MFCs the output was stable over time,
 220 however, when the feeding paused for ten days and cells left to starve, a different behavior
 221 was observed. Gelatin fed cells appeared to have better longevity as their performance
 222 gradually declined, and even for the first four days they had stable performance (**Fig. 5 -**
 223 **inset**). The rate of decrease of the positive control (urine) cells was the fastest among all the
 224 others with a decreasing trend of 0.73 $\mu\text{W}\cdot\text{h}^{-1}$. In all cases Nafion was consistently close to
 225 zero. The area under curve of the starvation period is presented in **Fig. 6B**.



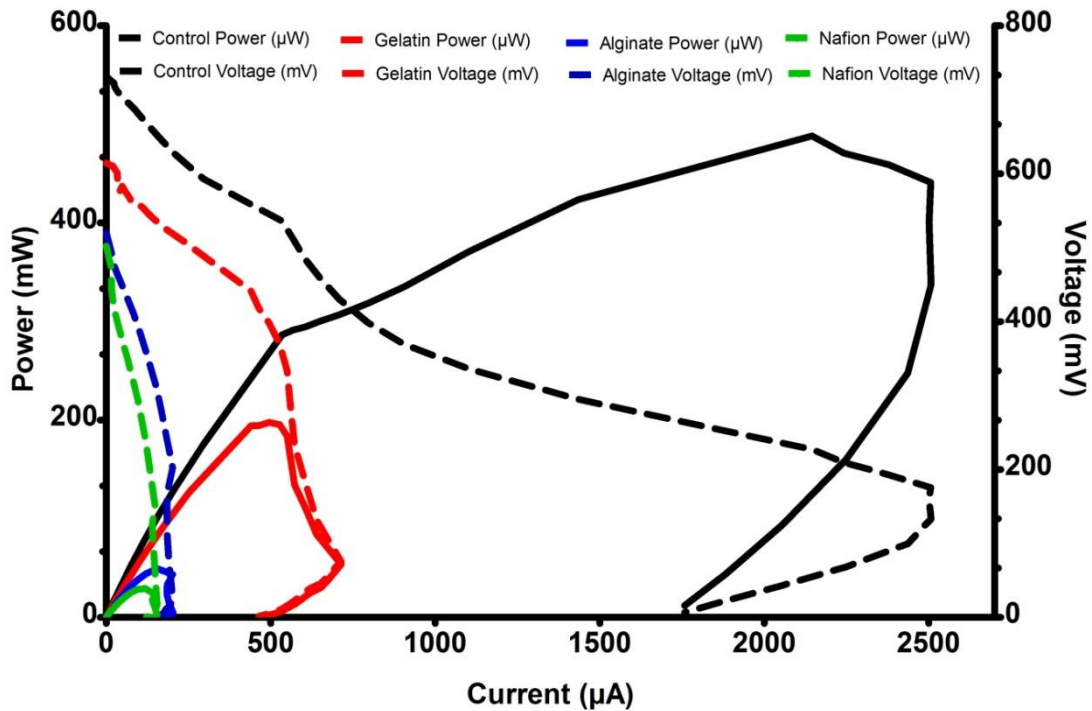
226 **Fig. 5 - Average power production of MFCs after feeding with different soft materials.**
 227 The highest absolute power output for the control was 149.23 μW and for the gelatin 111.26
 228 μW . Starvation period (total 10 days) is highlighted in the dotted box, a magnification of
 229 which is shown as the inset graph. Gelatin fed MFCs decreased at the slowest rate, which
 230 was the reason for its higher power output.



231 **Fig. 6 – Area under curve (AUC) of the full experiment (A) and the starvation period**
 232 **(B).**

233 3.4 Polarization Experiment

234 The polarization experiment was conducted two months after the start of the experiment. By
 235 this time the biofilm community was already well established and developed based on the
 236 2.7 k Ω load. Polarization power curves (**Fig. 7**) are consistent with the power output data
 237 (**Fig. 6**).



238

239 **Fig. 7 – Power curves produced after two months operation on a fixed load of 2.7 k Ω**

240 **4. Discussion**

241 **4.1 Clay membrane complications in batch mode**

242 Clay membranes possess a great advantage over the conventional proton exchange
 243 membranes (PEM) (eg. Nafion) because of their beneficial porosity, low cost, durability, as
 244 well as their ability to be 3D printed [19] [20]. On one hand, as the early results showed, the
 245 use of ceramic membrane in an open to the air batch mode fed MFC allow a significant
 246 percentage of water to be absorbed leaving the anode chamber almost dry having a
 247 detrimental effect on the performance. On the other hand, the always hydrated clay
 248 membrane in continuous flow offers a higher rate of proton/cation transfer [21] reflected by
 249 the higher output. Clay membranes have the potential to be extruded layer by layer from the
 250 Evobot platform, thus the three first steps of the custom made preparation of the membranes
 251 can be skipped.

252 **4.2 Polarization experiment**

253 The polarization experiment performed in this study was at the latter stage of the
 254 experiment, and cells were already operated at a stable resistance load. Studies suggest
 255 that early and regular polarisation experiments can determine the ideal resistance for
 256 maximum power production and by switching to that ideal load value the best power
 257 performance is achieved [22]. However other studies indicated that changing the external
 258 resistance does not improve the power output, as different combinations of microbial
 259 communities are developed based on each load that lead to comparable power outputs,
 260 showing the flexibility and resilience of MFC systems [23]. Thus, in this study it is believed
 261 that the unchanged load did not have a limiting effect on the MFCs' performance.

262 Nevertheless, an overshoot phenomenon was in fact observed in the polarization curves
263 [17]. The overshoot phenomenon occurs when there is either a delay in or a prevention of
264 charged molecules (ions and electrons) transfer, which results in decreasing the current at
265 the same time as the voltage. This overshoot may have therefore occurred due to the
266 complex nature of the substrates used (as well as the molecular weight/size) in conjunction
267 with the flow rate (resultant HRT), which appear to have resulted in high mass-transfer
268 (kinetic) losses. The power output recorded during the polarization experiments was much
269 higher (>3-fold) compared to the levels recorded in the real-time temporal curves. This might
270 be due to the short time of sampling (3 mins) during the polarization experiment, suggesting
271 that the period was not sufficiently long to reach steady-state conditions for identifying the
272 optimum resistance value for long-term experiments with a fixed load [17].

273 **4.3 Selection of target materials**

274 In this experiment gelatin, alginate and Nafion were tested as substrates with the prospect of
275 being used in the future as bacterial substrata or membranes for the 3D printed MFCs. Each
276 of these materials was selected because of its distinct properties. Gelatin and alginate are
277 biodegradable and all the materials tested are biocompatible. It is quite evident that gelatin is
278 a material that can be employed as both a substratum (3D extrude-able) and as a substrate
279 (microbially utilise-able), and this forms part of future work. Nafion was only used as a
280 negative control, due to its excellent ion-exchange properties, and the data show that if
281 employed in an EVOBOT line of work, it will need to be supplemented with a carbon-energy
282 substrate for sustaining bacterial growth.

283 **4.3.1 Alginate and gelatin**

284 Alginate or gelatin as well as pectin can be mixed with food proteins to be incorporated into
285 the 3D printing process [7]. For these reasons we tested alginate and gelatin as possible
286 printable feedstocks for the MFCs' bacterial community. This was due to the potential for
287 being 3D printed and blended with carbon energy sources, as well as immobilising bacterial
288 cells on an electrode surface and allowing their accumulation as a digesting biofilm.

289 Alginate is a polysaccharide and the second most abundant biopolymer in the world next to
290 cellulose [24], and it is composed of mannuronic and glucuronic acid residues which are
291 cross linked by calcium acids and form the ionotropic gel [7]. Alginate is derived from
292 seaweed and has been used as a useful cell-immobilising (entrapment) technique in
293 biotechnology due to its biocompatible properties as well as its ability to form heat-stable
294 gels that can be developed and set in room temperature [24]. Some species of bacteria can
295 hydrolyse alginate into cell transportable sugars with subsequent fermentation into short-
296 chain fatty acids [25].

297 Gelatin is an animal derived protein which has been known to be used as gelling agent in
298 early bacteriological media as a source of growth promoting substance [26]. However over
299 the years, agar based media proved more suitable for bacterial cultivation than gelatin based
300 media as gelatin cannot remain solid in temperatures above 37 °C (optimal condition for
301 pathogen growth) and it can be digested by many bacteria. Bacteria possessing the enzyme
302 gelatinase can break down gelatin into amino acids by hydrolyzing it [27]. Apart from their
303 biochemical and physiological characteristics, both gelatin and alginate powders are
304 considerably inexpensive substances (approximately £4-5/kg).

305 **4.3.2 Nafion**

306 Nafion is the main component of the commercially available proton exchange membranes
307 (PEM) for MFCs as it offers excellent thermal and mechanical stability as well as
308 conductivity. Nafion's high cost (liquid: £100/ 25 mL) though makes it an obstacle for MFCs
309 scale up and practical applications. In addition Nafion membranes require
310 activation/hydration prior to use and cannot be 3D printed, however the Nafion liquid mixed
311 with polymers, can be deposited from the EVOBOT platform into a solid layer and form a thin
312 layer of membrane. Even though, it is well known that Nafion is not a carbon energy source,
313 in this experiment it was used as feedstock for the purpose to identify if a jelly form nafion
314 membrane will cause biofouling [28] which is a common effect observed in Nafion
315 membranes (anode side) or have a detrimental effect on the bacterial community.

316 **4.4 Gelatin as 3D printable feedstock**

317 The long-chain polymer composition of gelatin and chitin renders the feedstock to be longer
318 lasting than monomeric substrates, which wash through the system or are quickly utilized.
319 Whereas proteolytic enzymes (such as gelatinase) are commonly encountered amongst
320 many different species of microorganism, the enzyme to hydrolyze chitin is thought to be
321 relatively rare, but encountered more in marine species. Gelatin's outperformance over the
322 other soft materials, and also its viscous characteristics make it a suitable material to be
323 employed into the 3D process towards the aim of monolithically fabricated MFCs which can
324 provide nutrients during a starving period or act as an endogenous store of fuel. The material
325 employed in the 3D process can be any soft material which can be easily extruded using a
326 RepRap EVOBOT machine and can also be used as a structural material.

327 **4.5 EvoBot and 3D printing**

328 The key to make MFCs more accessible is by simplifying the construction of MFCs through
329 the use of 3-dimensional (3D) fabrication techniques. The 3D printed/extruded MFCs will not
330 only speed up the manufacture of individual units, but can also help in automating the
331 production process of many units for scale-up. This will benefit the electrical power output as
332 rapidly fabricated multiple units can be stacked together to increase voltage or current output
333 [29]. It is envisaged that the EVOBOT machine will add a layer of nutrient agar – in the case
334 of flat surfaces – or continuously supplying nutrient broth – in the case of chambers – for
335 microbial growth and maintenance. Both, the nutrient agar on flat surfaces as well as the
336 nutrient broth for chambers, can be easily modified and supplied to the microbial
337 communities to test a wide variety of conditions, with the energy being the response of
338 selective pressure. The conductive element can be (initially) manually deposited, to allow the
339 bacteria to conduct electrons and then they can be extruded from the 3D printer as well. The
340 gelatin, as a feedstock and activated carbon paste as an electrode, serves the aim of the
341 experiment as a suitable alternative printable substratum and electron acceptor. The
342 optimised clay membrane can be extruded from the EVOBOT machine however at present
343 the kilning process required for the membrane to become durable and functional, is
344 prohibitive; other clay materials are currently being investigated.

345 **4.6 Future work**

346 This experiment can be optimised by feeding the fuel cells with feedstock that has been
347 standardised based on calorific value (even urine), rather than based on utilizable-energy

348 concentration. This may provide a clearer picture between alginate and gelatin. In addition,
349 alternatives for extrude-able membranes which do not require firing can be employed in
350 order to have the membrane ready to be used in the platform after extrusion. A next step can
351 be the extrusion of the materials through the EVOBOT syringe to form layer by layer a 3D
352 printed MFC prototype.

353 **5. Conclusion**

354 This experiment shows for the first time that entirely 3D printed MFCs have the potential to
355 be developed using the EVOBOT platform. Gelatin seems to be a promising soft material
356 that can be 3D printed and can be used as a feedstock for MFC operation. Flexible materials
357 such as ceramic clay used as a membrane, and activated carbon paste used as a cathode
358 electrode can be used in analytical type MFCs with the potential to be 3D-printed. Further
359 work will investigate different material combinations suitable for MFC fuel and
360 compartments, which could be used as part of an entirely 3D printable fuel cell.

361 **Acknowledgments**

362 The authors would like to thank the European Commission for the financial support of this
363 work through the FP7-ICT, grant agreement 611640 (EVOBLISS).

364

365

366

367 **References**

- 368 [1] Potter M. Electrical Effects Accompanying the Decomposition of Organic Compounds
 369 Published by : The Royal Society Electrical Effects accompanying the Decomposition
 370 of Organic. Proc R Soc London Ser B, Contain Pap a Biol Character, 1911;84:260–
 371 76.
- 372 [2] Bennetto HP. Electricity generation by microorganisms. *Biotechnol Educ* 1990;1:163–
 373 8.
- 374 [3] Nandy A, Kumar V, Mondal S, Dutta K, Salah M, Kundu PP. Performance evaluation
 375 of microbial fuel cells: Effect of varying electrode configuration and presence of a
 376 membrane electrode assembly. *N Biotechnol* 2015;32:272–81.
 377 doi:10.1016/j.nbt.2014.11.003.
- 378 [4] Logan B. *Microbial Fuel Cells*. Hoboken, New Jersey: John Wiley & Sons; 2008.
- 379 [5] Bennetto H, Mason JR, Stirling JL, Thurston CF. Miniature microbial biobatteries.
 380 *Power Sources* 1987;11:373–80.
- 381 [6] Hull C. Apparatus for production of three-dimensional objects by stereolithography,
 382 1984.
- 383 [7] Godoi FC, Prakash S, Bhandari BR. 3d printing technologies applied for food design:
 384 Status and prospects. *J Food Eng* 2016;179:44–54.
 385 doi:10.1016/j.jfoodeng.2016.01.025.
- 386 [8] Mitchell MG. Applications of 3D Printing in Cell Biology. *Cell Biol.*, Academic Press,
 387 Elsevier; 2016, p. 121–62. doi:10.1016/B978-0-12-801853-8.00002-8.
- 388 [9] Jonathan G, Karim A. 3D printing in pharmaceuticals: A new tool for designing
 389 customized drug delivery systems. *Int J Pharm* 2016;499:376–94.
 390 doi:10.1016/j.ijpharm.2015.12.071.
- 391 [10] Ledezma P, Ieropoulos I, Greenman J. Comparative analysis of different polymer
 392 materials for the construction of microbial fuel cell stacks. *J Biotechnol* 2010;150:143–
 393 143. doi:10.1016/j.jbiotec.2010.08.373.
- 394 [11] Ieropoulos I, Greenman J, Melhuish C, Horsfield I. EcoBot-III: a robot with guts. 12th
 395 *Int Conf Synth Simul Living Syst* 2010:733–40.
- 396 [12] Papaharalabos G, Greenman J, Melhuish C, Santoro C, Cristiani P, Li B, et al.
 397 Increased power output from micro porous layer (MPL) cathode microbial fuel cells
 398 (MFC). *Int J Hydrogen Energy* 2013;38:11552–8. doi:10.1016/j.ijhydene.2013.05.138.
- 399 [13] Philamore H, Rossiter J, Walters P, Winfield J, Ieropoulos I. Cast and 3D printed ion
 400 exchange membranes for monolithic microbial fuel cell fabrication. *J Power Sources*
 401 2015;289:91–9. doi:10.1016/j.jpowsour.2015.04.113.
- 402 [14] Zhao C, Wang C, Gorkin R, Beirne S, Shu K, Wallace GG. Three dimensional (3D)
 403 printed electrodes for interdigitated supercapacitors. *Electrochem Commun*
 404 2014;41:20–3. doi:10.1016/j.elecom.2014.01.013.
- 405 [15] Faíña A, Nejatimoharrami F, Stoy K. EvoBot: An Open-Source, Reactive Liquid
 406 Handling Robot. *IEEE/RSJ Int. Conf. Intell. Robot. Syst.*, 2015.
- 407 [16] Gajda I, Greenman J, Melhuish C, Ieropoulos I. Simultaneous electricity generation
 408 and microbially-assisted electrosynthesis in ceramic MFCs. *Bioelectrochemistry*
 409 2015;104:58–64. doi:10.1016/j.bioelechem.2015.03.001.
- 410 [17] Winfield J, Ieropoulos I, Greenman J, Dennis J. The overshoot phenomenon as a
 411 function of internal resistance in microbial fuel cells. *Bioelectrochemistry* 2011;81:22–
 412 7. doi:10.1016/j.bioelechem.2011.01.001.
- 413 [18] Degrenne N, Buret F, Allard B, Bevilacqua P. Electrical energy generation from a

- 414 large number of microbial fuel cells operating at maximum power point electrical load.
415 J Power Sources 2012;205:188–93. doi:10.1016/j.jpowsour.2012.01.082.
- 416 [19] 3dprint.com 2015.
- 417 [20] Herpt O. Functional 3D Printed Ceramics - Olivier van Herpt. 2016.
- 418 [21] Ghadge AN, Sreemannarayana M, Duteanu N, Ghangrekar M. Influence of ceramic
419 separator's characteristics on microbial fuel cell performance. J Electrochem Sci Eng
420 2014;4:315–26. doi:10.5599/jese.2014.
- 421 [22] Lovley DR. The microbe electric: conversion of organic matter to electricity. Curr Opin
422 Biotechnol 2008;19:564–71. doi:10.1016/j.copbio.2008.10.005.
- 423 [23] Lyon DY, Buret F, Vogel TM, Monier J-M. Is resistance futile? Changing external
424 resistance does not improve microbial fuel cell performance. Bioelectrochemistry
425 2010;78:2–7. doi:10.1016/j.bioelechem.2009.09.001.
- 426 [24] Melvik JE, Dornish M. Alginate as a Carrier for Cell Immobilisation. Fundam. Cell
427 Immobil. Biotechnol., 2004, p. 33–51.
- 428 [25] Michel C, Lahaye M, Bonnet C, Mabeau S, Barry JL. In vitro fermentation by human
429 faecal bacteria of total and purified dietary fibres from brown seaweeds. Br J Nutr
430 1996;263–80. doi:10.1079/BJN19960129.
- 431 [26] Koser SA, Chinn BEND, Saunders F. Gelatin as a source of growth-promoting
432 substances for bacteria. J Bacteriol 1938;36:57–65.
- 433 [27] Levine, M Carpenter DC. Gelatin liquefaction by bacteria. J Bacteriol 1922;8:297–306.
- 434 [28] Chae K, Choi M, Ajayi F, Park W. Mass transport through a proton exchange
435 membrane (nafion) in microbial fuel cells†. Energy & Fuels 2008;22:169–76.
436 doi:10.1021/ef700308u.
- 437 [29] Ledezma P, Stinchcombe A, Greenman J, Ieropoulos I. The first self-sustainable
438 microbial fuel cell stack. Phys Chem Chem Phys 2013;15:2278–81.
439 doi:10.1039/c2cp44548d.
- 440